engineering proceedings

MDPI

Proceeding Paper

Comparative Analysis of the Interaction of Cytochrome C with Supported Lipid Films and DNA Aptamers Using QCM-D Method †

Marek Tatarko *, Sandro Spagnolo, Martin Csiba, Veronika Šubjaková and Tibor Hianik

Department of Nuclear Physics and Biophysics, Faculty of Mathematics, Physics and Informatics, Comenius University in Bratislava, Mlynska dolina F1, 84248 Bratislava, Slovakia; spagnolo2@uniba.sk (S.S.); csiba17@uniba.sk (M.C.); veronika.subjakova@fmph.uniba.sk (V.Š.); tibor.hianik@fmph.uniba.sk (T.H.)

* Correspondence: tatarko4@uniba.sk

† Presented at the 3rd International Electronic Conference on Biosensors, 8–21 May 2023; Available online: https://iecb2023.sciforum.net.

Abstract: Cytochrome c (cyt c) is an important indicator of cell apoptosis and can, therefore, be used for the diagnosis of cancer. We performed a comparative analysis of cyt c detection on the surface of lipid films or a monolayer of 11-mercaptoundecanoic acid (MUA) with immobilized specific or nonspecific DNA aptamers. A quartz crystal microbalance with dissipation monitoring (QCM-D) in a multiharmonic mode was used to study the interaction of cyt c with various surfaces. For this purpose, changes in the resonant frequency, Δf, and dissipation, ΔD, were determined. The strongest interaction of cyt c was observed with sensors based on specific DNA aptamers that were accompanied by a decrease in frequency and an increase in dissipation. The limit of detection (LOD) for this aptasensor was established as 2.89 ± 0.12 nM. The interaction of cyt c with supported lipid films also resulted in a decrease in resonant frequency, but significant changes occurred only in the μM concentration range of cyt c. Changes in dissipation were much lower in comparison with aptamer-based surfaces, which suggests a weaker contribution of cyt c adsorption to the viscosity.

Keywords: cytochrome c; biosensor; lipid films; DNA aptamers; QCM-D

Citation: Tatarko, M.; Spagnolo, S.; Csiba, M.; Šubjaková, V.; Hianik, T. Comparative Analysis of the Interaction of Cytochrome C with Supported Lipid Films and DNA Aptamers Using QCM-D Method. *Eng. Proc.* **2023**, *35*, 35. https://doi.org/10.3390/IECB2023-14752

Academic Editor: Evgeny Katz

Published: 12 June 2023

1. Introduction

Cytochrome c (cyt c) belongs to the most essential proteins in living organisms. This relatively small hemoprotein (molecular weight of 12 kDa, diameter of 5 nm) has a significant role in electron transport in mitochondria. It is positively charged and has redox properties [1], which are often used in electrochemical studies [2]. Cyt c also plays an important role in cell apoptosis, which is accompanied by the release of cyt c from the mitochondrial membrane to the cytoplasm [3,4]. Therefore, the detection of cyt c can serve as a suitable tool for evaluating the effectiveness of chemotherapy. The monitoring of cell apoptosis during chemotherapy can prevent undesirable damage to healthy tissues [5,6].

Standard methods of cyt c detection, such as flow cytometry, enzyme-linked immunosorbent assay (ELISA), and high-performance liquid chromatography (HPLC), are commonly used for cyt c detection [7]. However, these methods are time consuming and require expensive instruments and well-trained personnel. Current trends in cyt c detection are focused on the application of biosensors based on DNA aptamers as receptors [8]. Aptamers are relatively short single-stranded RNA or DNA (typically around 30–80 bases) that are selected by combinatorial chemistry known as SELEX (systematic evolution of ligands by exponential enrichment) [9,10]. Using this method, the DNA aptamers specific to cyt c were developed. However, because cyt c is positively charged, interaction with negatively charged DNA aptamers can also be non-specific due to electrostatic binding. DNA aptamers, as an alternative to more expensive and less stable antibodies [7],

were used for the development of several biosensors for cyt c detection [11,12]. Recent research reports the sub-nanomolar limit of detection (LOD) of cyt c for electrochemical and acoustic biosensors [13].

An analysis of the mechanisms of these interactions requires certain model studies. Cyt c can be immobilized on the surface of supported lipid films bearing a negative charge, or covalently immobilized on the monolayers of 11-mercaptoundecanoic acid (MUA), as reported in our recent work [14]. Using a quartz crystal microbalance with dissipation monitoring (QCM-D), we have shown that cyt c is released from the surface of lipid films following interaction with DNA aptamers. As a result, the resonant frequency increased. However, when cyt c was covalently attached to the surface of MUA, the frequency decreased, which is evidence of the formation of an aptamer binding layer on the surface. However, it is still not clear how to eliminate the specific and non-specific binding of cyt to the negatively charged DNA aptamers and other molecules or structures such as lipid films. So far, such a comparative analysis of cyt c binding has not been reported. Therefore, in this work, we extended our studies recently published in [14] on the analysis of the changes in the resonant frequency, Δf, and dissipation, ΔD, following the adsorption of cyt c in the MUA layers modified by specific or nonspecific aptamers, as well as with supported lipid films and those with the adsorbed model protein bovine serum albumin.

2. Materials and Methods

2.1. Chemicals

The experiments were performed using phosphate-buffered saline (PBS) composed of 10 mM Na_2HPO_4, 1.8 mM KH_2PO_4, 137 mM NaCl, 2.7 mM KCl, and pH 7.4. We also used phosphate buffer (PB) (10 mM Na_2HPO_4, 1.8 mM KH_2PO_4) containing 2 mM $MgCl_2$. MiliQ water with a resistance of 18 MΩ·cm prepared by Purelab Classic UV (Elga, High Wycombe, UK) was used for the preparation of all aqueous solutions. The standard chemicals, such as ethanol, NaCl, HNO_3, NH_3, H_2O_2, $MgCl_2$, and $CaCl_2$, were purchased from Slavus (Bratislava, Slovakia). The supported lipid membranes were prepared by liposome fusion from 1,2-dimyristoyl-sn-glycero-3-phosphocholine (DMPC) (Avanti Polar Lipids Inc., Birmingham, AL, USA) and 1,2-Dimyristoyl-sn-glycero-3-phospho-rac-(1-glycerol) sodium salt (DMPG) (Sigma Aldrich, Darmstadt, Germany). 1-dodecanethiol (DDT), 11-mercapto-1-undecanoic acid (MUA), bovine serum albumin (BSA), *N*-(3-Dimethylaminopropyl)-N′-ethylcarbodiimide hydrochloride (EDC), and *N*-Hydroxysuccinimide (NHS) were purchased from Sigma Aldrich (Darmstadt, Germany). DNA aptamers sensitive to cyt c were purchased from Biosearch Technologies (Risskov, Denmark). The aptamers were modified by the amino groups at the 5′ ends (NH_2-Apt-cytc) and had the following sequence [15]: 5′-NH_2-TTTTTTTTTTATCGATAAGCTTCCAGAGCCGTGTCTGGGGCCGACCGGCGCATTGGGTACGTTGTTGCCGTAGAATTCCTGCAGCC-3′. A 10-mer thymidine spacer at the 5′ ends was included to improve conformational flexibility. We also used a DNA aptamer that did not specifically bind to cyt c with the following sequence: 5′-NH_2-CTGAATTGGATCTCTCTTCTTGAGCGATCTCCACA-3′. The aptamer was purchased from Generi Biotech Ltd. (Hradec Králové, Czech Republic).

2.2. Preparation of Aptamer-Based Sensing Surfaces, Supported Lipid Films and QCM-D Measurements

The lipid films and other layers were prepared on the surface of an 8 MHz AT-cut quartz crystal with a working area of 0.2 cm^2 consisting of a thin gold layer (Total Frequency Control Ltd., Storrington, UK). Before lipid application, the crystal was incubated for 16 h at room temperature in 2 mM 1-dodecanthiol (DDT) in ethanol. The modified crystal was placed in an acrylic flow cell (JKU, Linz, Austria) connected to a syringe pump (Genie Plus, Kent Scientific, Torrington, CT, USA). The frequency, Δf, and dissipation, ΔD, changes were measured using a computer-controlled vector analyzer Sark 110 (Seeed, Shenzhen, China). Lipid films were prepared by the fusion of liposomes. Small unilamellar liposomes (diameter approximately 20 nm) were prepared by the sonication of the lipid solution in

PB. For this purpose, an 8 mg mixture of phospholipids (equimolar ratio of DMPC: DMPG) was dissolved in a small volume of chloroform in a round glass flask. Chloroform was then evaporated by a gentle stream of nitrogen, and the constant circular motion of the flask caused the deposition of the lipid film on its wall. An aliquot containing PB was then added and incubated for 30 min. Incubation was followed by ultrasonication for 20 min at room temperature in the sonicator (Bandelin Sonorex RK31, Berlin, Germany) [15]. The final liposome solution with a concentration of 0.5 mg/mL was then applied by a flow on the surface of a DDT-modified gold layer of the quartz crystal. The MUA layer on a quartz crystal surface was prepared by chemisorption from 2 mM MUA during a 16 h incubation. The crystals were then washed with MiliQ water and incubated for 35 min in a 20 mM EDC and 50 mM NHS mixture to activate the carboxylic group of MUA. The aptamer layers were formed by the addition of 1 µM aptamers to the surface of MUA activated by NHS/EDC. This resulted in covalent immobilization of the aptamers [16].

Cyt c was added in the flow mode (flow rate 50 µL/min) to the surface of lipid films or aptamer layers at various concentrations. Changes in resonant frequency, Δf, caused by the adsorption of cyt c were evaluated using the Sauerbrey equation [17]

$$\Delta f = \frac{-2nf_0^2}{\sqrt{\rho_q \mu_q}} \frac{\Delta m}{A} \quad (1)$$

where n represents the harmonic number, f_0 is fundamental resonance frequency, Δm is mass change, A is the working area of the crystal (0.2 cm^2), μ_q is the shear modulus of elasticity (2.947 × 10^{11} g·cm^{-1}·s^{-2}), and ρ_q is the density of the crystal (2.648 g·cm^{-3}).

3. Results and Discussion

In the first series of experiments, we studied the changes in the frequency, Δf, and dissipation, ΔD, following the addition of cyt c to the layers formed by NH_2-aptamers covalently immobilized on the MUA layer. The remaining amino-reactive MUA sites were blocked by BSA. The kinetics of the frequency and dissipation changes following the addition of BSA and cyt c for the third to ninth harmonics are shown in Figure 1. A decrease in the resonant frequency and an increase in the dissipation can be seen.

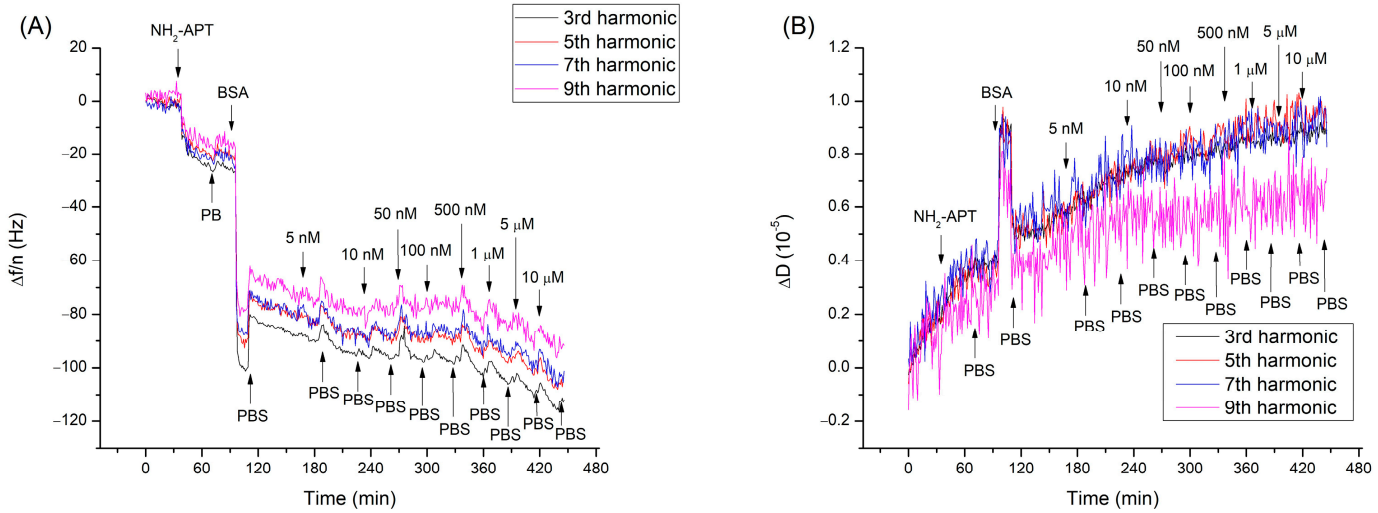

Figure 1. The kinetics of the 3rd to 9th harmonic frequencies, $\Delta f/n$, normalized by harmonic number (**A**) and dissipation ΔD (**B**) following the addition of specific DNA aptamers (NH_2-APT), BSA, and cyt c in the concentration range of 5 nM–10 µM on the MUA layer chemisorbed on the thin gold layer of the piezo crystal. The moments of addition of aptamers, BSA, cyt c, and PBS wash are shown by arrows.

We also performed similar experiments on the supported lipid membranes. In the experiments, we used PB containing 2 mM $MgCl_2$. The kinetics of the changes in the normalized frequency and dissipation following the addition of various concentrations of cyt c are shown in Figure 2.

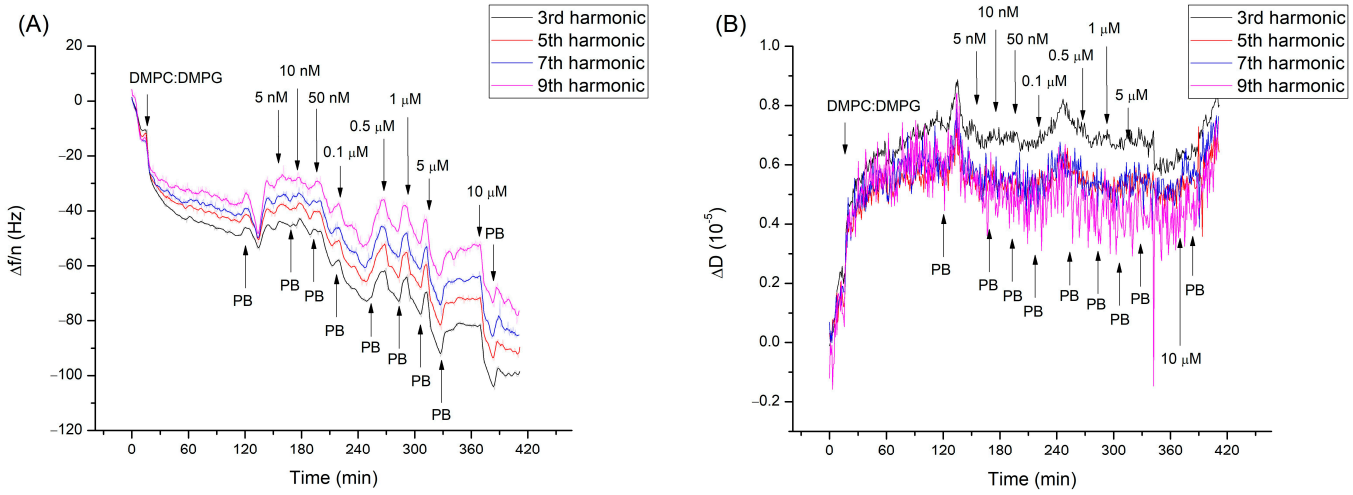

Figure 2. The kinetics of the 3rd to 9th harmonic frequencies, $\Delta f/n$, normalized by harmonic number (**A**) and dissipation ΔD (**B**) following the addition of DMPC:DMPG liposomes (0.5 mg/mL) and cyt c in the concentration range 5 nM–10 μM on the chemisorbed layer of DDT on the gold surface of the piezo crystal. The moments of addition of liposomes, cyt c, and PB wash are shown by arrows.

As can be seen, substantial changes in the acoustic values occurred following the addition of cyt c in the μM concentrations. We also tested the interaction of cyt c with the surface formed by nonspecific DNA aptamers and BSA immobilized on the MUA monolayer. Specific and nonspecific interactions of cyt c with the aptamers resulted in similar changes in the acoustic parameters. Much lower changes in frequency and dissipation were observed for the interaction of cyt c with BSA covalently immobilized on the MUA monolayer. The plot of the changes in frequency (A) and dissipation (B) vs. concentration of cyt c for various surfaces studied is shown in Figure 3. The obtained results suggest that there is increased adsorption of cyt c on the surface formed by specific DNA aptamers. Cyt c also interacted with the surfaces formed by nonspecific aptamers or BSA, but the frequency changes were lower. The estimated limit of detection (LOD) for cyt c using specific aptamers was 2.89 ± 0.12 nM. It is higher than the value reported by Poturnayova et al. [18] (0.50 ± 0.05 nM). However, in this study, the sensor was formed by biotinylated aptamers attached to the neutravidin layer. It can also be seen that with increasing concentration of cyt c, the dissipation substantially increased for aptamer-based sensors, whereas practically no changes in this value occurred for lipid layers as well as for BSA. In the latter case, however, a sharp increase in dissipation occurred at a rather high cyt c concentration (10 μM). Substantial changes in dissipation for the interaction of cyt c with aptamer layers can be due to the influence of cyt c on the conformation and flexibility of aptamers. At the same time, cyt c on the surface of lipid films probably forms a tightly packed rigid protein layer that practically does not contribute to the surface viscosity.

Using the Sauerbrey equation, we also compared the surface density of cyt c at different surfaces and at the maximally applied cyt c concentrations of 10 μM. The results of the calculations are presented in Table 1. Based on the frequency changes, we first calculated the surface density and then the number of molecules that were adsorbed on the surface. As can be seen, the surface density of cyt c on specific aptamers is 3.7 times higher than the surface density of these aptamers. Considering that the specific aptamer probably has one binding site for cyt c, the larger number of adsorbed cyt c molecules could also be due to non-specific interactions between positively charged cyt c and negatively charged aptamers. It can also be seen that the surface density of cyt c is only slightly higher for

specific aptamers in comparison with non-specific ones. This is an additional confirmation of the existence of non-specific interactions between cyt c and aptamers. The adsorption of cyt c on the lipid membrane was the most extensive and resulted in a cyt c surface density of (18.73 ± 2.88) × 10^{12} molecules·cm^{-2}. Considering that changes in dissipation for lipid films were rather small, one can assume that the Sauerbrey equation can be used more correctly in comparison with the sensing layers based on aptamers. In the latter case, viscosity contribution to the frequency changes can cause an overestimated frequency decrease. This means that the real surface density of cyt c at such a surface can be lower than that shown in Table 1.

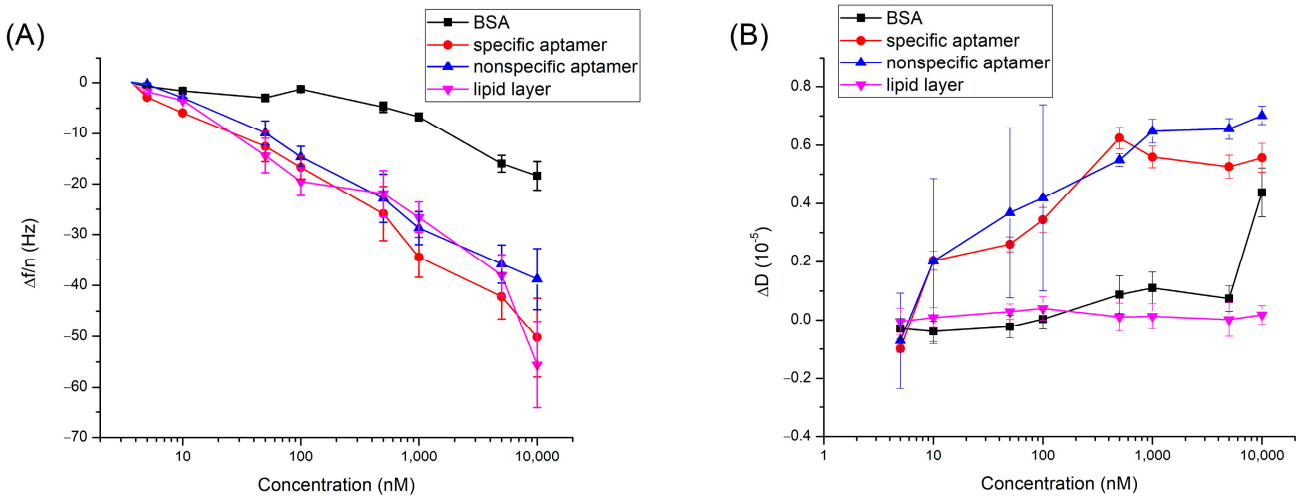

Figure 3. The plot of the changes in resonant frequency $\Delta f/n$ (**A**) and dissipation ΔD (**B**) vs. cyt c concentration for surfaces based on physically adsorbed BSA on a gold surface (black), specific aptamer (red), nonspecific aptamer (blue), and mixed lipid layer (purple). Measurements were performed in PB. The results are mean ± S.D. obtained for at least 3 independent measurements in each system.

Table 1. The frequency changes, Δf, mass density, $\Delta m/A$, and surface concentrations of molecules, σ, were calculated using the Sauerbrey equation for the systems studied. For calculation, we used the molecular weight of BSA (66 kDa), specific aptamer (26.165 kDa), nonspecific aptamer (10.647 kDa), and cyt c (12.327 kDa). The surface density of the molecules was calculated as mass density × (N_A/Mw), where N_A is Avogadro's number (6.02205 × 10^{23} mol^{-1} and Mw is the molecular weight.

Adsorbed Molecule	Δf (Hz)	$\Delta m/A$ (μg·cm^{-2})	σ (10^{12} cm^{-2})
BSA (on MUA)	−47.67 ± 2.4	0.33 ± 0.02	3.00 ± 0.15
Specific apt. (on MUA)	−28.75 ± 4.14	0.20 ± 0.03	4.57± 0.66
Non-specific apt. (on MUA)	−10.15 ± 4.40	0.07 ± 0. 03	3.96 ± 1.72
Cyt c (on BSA)	−18.38 ± 2.80	0.13 ± 0.19	6.20 ± 0.94
Cyt c (on specific apt.)	−50.21 ± 7.70	0.35 ± 0.05	16.92 ± 2.59
Cyt c (on non-specific apt.)	−38.75 ± 5.96	0.27 ± 0.41	13.06 ± 2.01
Cyt c (on lipid film)	−55.58 ± 8.55	0.38 ± 0.59	18.73 ± 2.88

4. Conclusions

In this study, we demonstrated that cyt c interacts with both specific and non-specific DNA aptamers covalently attached to the MUA layers. The surface density was, however, slightly higher for specific aptamers. The fact that cyt c interacts rather strongly with non-specific aptamers is challenging. This phenomenon requires further analysis. The mixed DMPC/DMPG monolayers also revealed high adsorption of cyt c. This effect can be used to further study the detection of cyt c on the lipid surface by nanowires, for example, modified by DNA aptamers.

Author Contributions: Conceptualization T.H.; formal analysis, M.T., S.S. and T.H.; investigation, M.T., S.S., M.C. and V.Š.; methodology, M.T., S.S., V.Š. and T.H.; validation, M.T., M.C. and V.Š.; funding acquisition, T.H.; project administration, T.H.; supervision, T.H.; writing—original draft, M.T., S.S., V.Š. and T.H.; writing—review and editing, M.T. and T.H. All authors have read and agreed to the published version of the manuscript.

Funding: This work has received funding from the Science Grant Agency VEGA, project number: 1/0445/23.

Institutional Review Board Statement: Not applicable.

Informed Consent Statement: Not applicable.

Data Availability Statement: Not applicable.

Conflicts of Interest: The authors declare no conflict of interest.

References

1. Geng, R.; Zhao, G.; Liu, M.; Li, M. A sandwich structured SiO_2/cytochrome c/SiO_2 on a boron-doped diamond film electrode as an electrochemical nitrite biosensor. *Biomaterials* **2008**, *29*, 2794–2901. [CrossRef] [PubMed]
2. Lee, T.; Kim, S.-U.; Lee, J.-H.; Min, J.; Choi, J.-W. Fabrication of nano scaled protein monolayer consisting of cytochrome c on self-assembled 11-MUA layer for bioelectronic device. *J. Nanosci. Nanotechnol.* **2009**, *9*, 7136–7140. [CrossRef] [PubMed]
3. Martinou, J.C.; Desagher, S.; Antonsson, B. Cytochrome c release from mitochondria: All or nothing. *Nat. Cell Biol.* **2000**, *2*, 41–43. [CrossRef] [PubMed]
4. Goldstein, J.C.; Waterhouse, N.J.; Juin, P.; Evan, G.I.; Green, D.R. The coordinate release of cytochrome c during apoptosis is rapid, complete and kinetically invariant. *Nat. Cell Biol.* **2000**, *2*, 156–162. [CrossRef] [PubMed]
5. Eleftheriadis, T.; Pissas, G.; Liakopoulos, V.; Stefanidis, I. Cytochrome c as a potentially clinical useful marker of mitochondrial and cellular damage. *Front. Immunol.* **2016**, *7*, 279. [CrossRef] [PubMed]
6. Yadav, S.; Sawarni, N.; Kumari, P.; Sharma, M. Advancement in analytical techniques fabricated for the quantitation of cytochrome c. *Process Biochem.* **2022**, *122*, 315–330. [CrossRef]
7. Manickam, P.; Kaushik, A.; Karunakaran, C.; Bhansali, S. Recent advances in cytochrome c biosensing technologies. *Biosens. Bioelectron.* **2017**, *87*, 654–668. [CrossRef] [PubMed]
8. Subjakova, V.; Oravczova, V.; Hianik, T. Polymer nanoparticles and nanomotors modified by DNA/RNA aptamers and antibodies in targeted therapy of cancer. *Polymers* **2021**, *13*, 341. [CrossRef] [PubMed]
9. Zhou, W.; Huang, P.-J.J.; Ding, J.; Liu, J. Aptamer-based biosensors for biomedical diagnostics. *Analyst* **2014**, *139*, 2627–2640. [CrossRef] [PubMed]
10. He, F.; Wen, N.; Xiao, D.; Yan, J.; Xiong, H.; Cai, S.; Liu, Z.; Liu, Y. Aptamer-based targeted drug delivery systems: Current potential and challenges. *Curr. Med. Chem.* **2020**, *27*, 2189–2219. [CrossRef] [PubMed]
11. Jalalvand, A.R.; Akbari, V.; Bahramikia, S. Two- and multi-way analyses of cardiolipin-cytochrome c interactions and exploiting second-order advantage for bio-sensing of cytochrome c. *Sens. Bio-Sens. Res.* **2022**, *38*, 100518. [CrossRef]
12. Stepanova, V.B.; Shurpik, D.N.; Evtugyn, V.G.; Stoikov, I.I.; Evtugyn, G.A.; Osin, Y.N.; Hianik, T. Label-free electrochemical aptasensor for cytochrome c detection using pillar[5]arene bearing neutral red. *Sens. Actuators B Chem.* **2016**, *225*, 57–65. [CrossRef]
13. Poturnayova, A.; Leitner, M.; Snejdarkova, M.; Hinterdorfer, P.; Hianik, T.; Ebner, A. Molecular addressability of lipid membrane embedded calixarenes towards cytochrome c. *J. Nanomed. Nanotechnol.* **2014**, *5*, 202. [CrossRef]
14. Tatarko, M.; Spagnolo, S.; Csiba, M.; Šubjaková, V.; Hianik, T. Analysis of the interaction between DNA aptamers and cytochrome c on the surface of lipid films and on the MUA monolayer: A QCM-D study. *Biosensors* **2023**, *13*, 251. [CrossRef] [PubMed]
15. Mirsky, V.M.; Muss, M.; Krause, C.; Wolfbeis, O.S. Capacitive approach to determine phospholipase A2 activity toward artificial and natural substrates. *Anal. Chem.* **1998**, *70*, 3674–3678. [CrossRef] [PubMed]
16. Chinnapen, D.J.; Sen, D. Hemin-stimulated docking of cytochrome c to a hemin-DNA aptamer complex. *Biochemistry* **2002**, *41*, 5202–5212. [CrossRef] [PubMed]
17. Sauerbrey, G. Verwendung von schwingquarzen zur wägung dünner schichten und zur mikrowägung. *Z. Phys.* **1959**, *155*, 206–222. [CrossRef]
18. Poturnayova, A.; Castillo, G.; Subjakova, V.; Tatarko, M.; Snejdarkova, M.; Hianik, T. Optimization of cytochrome c detection by acoustic and electrochemical methods based on aptamer sensors. *Sens. Actuators B Chem.* **2017**, *238*, 817–827. [CrossRef]